



ELSEVIER

Contents lists available at ScienceDirect

NeuroImage: Clinical

journal homepage: [www.elsevier.com/locate/ynicl](http://www.elsevier.com/locate/ynicl)

## Migraine with aura in women is not associated with structural thalamic abnormalities



Anders Hougaard<sup>a,1</sup>, Silas Haahr Nielsen<sup>b,1</sup>, David Gaist<sup>c,d</sup>, Oula Puonti<sup>b</sup>, Ellen Garde<sup>b</sup>, Nina Linde Reisleiv<sup>b</sup>, Pernille Iversen<sup>b</sup>, Camilla Gøbel Madsen<sup>b,e</sup>, Morten Blaabjerg<sup>c,d</sup>, Helle Hvilsted Nielsen<sup>c,d</sup>, Thomas Krøigård<sup>c,d</sup>, Kamilla Østergaard<sup>c,d</sup>, Kirsten Ohm Kyvik<sup>d,f,g</sup>, Kristoffer Hougaard Madsen<sup>b,h</sup>, Hartwig Roman Siebner<sup>b,i,j</sup>, Messoud Ashina<sup>a,j,\*</sup>

<sup>a</sup> Danish Headache Center, Department of Neurology, Rigshospitalet Glostrup, Faculty of Health and Medical Sciences, University of Copenhagen, Denmark

<sup>b</sup> Danish Research Centre for Magnetic Resonance, Copenhagen University Hospital Hvidovre, Hvidovre, Denmark

<sup>c</sup> Department of Neurology, Odense University Hospital, Denmark, Odense, Denmark

<sup>d</sup> Department of Clinical Research, Faculty of Health Sciences, University of Southern Denmark, Odense, Denmark

<sup>e</sup> Department of Radiology, Centre for Functional and Diagnostic Imaging and Research, Copenhagen University Hospital Amager and Hvidovre, Hvidovre, Denmark

<sup>f</sup> The Danish Twin Registry, Epidemiology, Biostatistics and Biodemography, Institute of Public Health, University of Southern Denmark, Odense, Denmark

<sup>g</sup> Odense Patient data Explorative Network (OPEN), Odense University Hospital, Odense, Denmark

<sup>h</sup> Department of Applied Mathematics and Computer Science, Technical University of Denmark, Kgs. Lyngby, Denmark

<sup>i</sup> Department of Neurology, Copenhagen University Hospital Bispebjerg, Copenhagen, Denmark

<sup>j</sup> Department of Clinical Medicine, Faculty of Medical and Health Sciences, University of Copenhagen, Copenhagen, Denmark

### ARTICLE INFO

#### Keywords:

Headache  
Thalamus  
Structure  
Volume  
Nuclei  
Population-based

### ABSTRACT

Migraine with aura is a highly prevalent disorder involving transient neurological disturbances associated with migraine headache. While the pathophysiology is incompletely understood, findings from clinical and basic science studies indicate a potential key role of the thalamus in the mechanisms underlying migraine with and without aura. Two recent, clinic-based MRI studies investigated the volumes of individual thalamic nuclei in migraine patients with and without aura using two different data analysis methods. Both studies found differences of thalamic nuclei volumes between patients and healthy controls, but the results of the studies were not consistent.

Here, we investigated whether migraine with aura is associated with changes in thalamic volume by analysing MRI data obtained from a large, cross-sectional population-based study which specifically included women with migraine with aura (N = 156), unrelated migraine-free matched controls (N = 126), and migraine aura-free co-twins (N = 29) identified from the Danish Twin Registry. We used two advanced, validated analysis methods to assess the volume of the thalamus and its nuclei; the MAGEt Brain Algorithm and a recently developed FreeSurfer-based method based on a probabilistic atlas of the thalamic nuclei combining ex vivo MRI and histology. These approaches were very similar to the methods used in each of the two previous studies.

Between-group comparisons were corrected for potential effects of age, educational level, BMI, smoking, alcohol, and hypertension using a linear mixed model. Further, we used linear mixed models and visual inspection of data to assess relations between migraine aura frequency and thalamic nuclei volumes in patients. In addition, we performed paired t-tests to compare volumes of twin pairs (N = 29) discordant for migraine with aura. None of our analyses showed any between-group differences in volume of the thalamus or of individual thalamic nuclei. Our results indicate that the pathophysiology of migraine with aura does not involve alteration of thalamic volume.

\* Corresponding author at: Danish Headache Center, Department of Neurology, Rigshospitalet Glostrup, Valdemar Hansens Vej 5, DK-2600 Glostrup, Denmark.  
E-mail address: [ashina@dadlnet.dk](mailto:ashina@dadlnet.dk) (M. Ashina).

<sup>1</sup> These authors contributed equally to this work.

<https://doi.org/10.1016/j.nicl.2020.102361>

Received 28 March 2020; Received in revised form 6 July 2020; Accepted 9 July 2020

Available online 25 July 2020

2213-1582/ © 2020 The Authors. Published by Elsevier Inc. This is an open access article under the CC BY-NC-ND license

(<http://creativecommons.org/licenses/by-nc-nd/4.0/>).

## 1. Introduction

Migraine with aura is a complex brain disorder presenting clinically as attacks of transient neurological symptoms, mostly characteristic visual or somatosensory disturbances (Headache Classification Committee of the International Headache Society, 2018). The symptoms are typically followed by head pain accompanied by photo- and phonophobia, i.e. the headache phase of the migraine attack. The pathophysiological mechanisms of this highly prevalent and disabling condition are not well understood. While the migraine aura symptoms *per se* are believed to be caused by a slowly propagating wave of gray matter depolarization, so called spreading depolarization (SD), it remains elusive why patients suffering from this disorder apparently are more susceptible to SD and the relation to the subsequent headache and associated symptoms is not clear (Charles and Hansen, 2015).

The thalamus is a nuclear complex located in the diencephalon between the midbrain and cortex. It has a critical role in relaying and modulating sensory information travelling from the periphery to the cortex. Recent data from pre-clinical and clinical studies suggest that the thalamus could play a key role in the disease mechanisms of migraine with and without aura (Younis et al., 2018). More specifically, dysfunction of thalamocortical connections have been proposed to explain the increased sensitivity to pain and other sensory stimuli, as well as a reduced threshold for SD elicitation, in migraine (de Tommaso et al., 2014; Helms and Dechent, 2009). The clinical features in migraine of photophobia (Griswold et al., 2002; Nosedá et al., 2016) and allodynia (Burstein et al., 2010) have also been suggested to depend on thalamic dysfunction. A multi-center MRI study investigating the volume of thalamic nuclei in 131 migraine patients (38 with aura) (Magon et al., 2015) reported a reduced volume of several thalamic nuclei in patients compared to healthy controls, including the central nuclear complex, anterior nucleus and lateral dorsal nucleus. The authors suggested that the findings were indicative of abnormal processing of the affective and cognitive components of pain in migraine. The volume differences were not found when investigating the subgroups of migraine patients with and without aura specifically, possibly due to lack of statistical power. In contrast, another recent clinic-based study, using a different data analysis method, found increased volumes of the medial geniculate and anteroventral nuclei in migraine patients without aura compared to healthy controls (Shin et al., 2019).

To investigate whether migraine with aura is associated with changes in thalamic volume, we analysed MRI data obtained from a large, cross-sectional population-based study which specifically included migraine patients with aura. We used two advanced, validated, complimentary analysis methods, i.e. both of the methods used in the two previous, abovementioned studies, to assess the volume of the thalamus and its nuclei. We sought to determine whether any of the previously reported abnormalities of thalamic nuclei volumes could be identified in a large sample of migraine patients with aura specifically.

## 2. Methods

We based our analyses on data from the Women with Migraine with Aura Neuroimaging (WOMAN) study, which has previously been presented in detail (Gaist et al., 2016, 2018). In brief, we used the Danish Twin Registry (Skytthe et al., 2006), to recruit female twins born 1931 to 1982, who based on earlier responses to a previously used questionnaire

Gaist et al. (2005) were classified as screen positive for migraine with aura, co-twins to females screen positive to migraine with aura, or screen negative for migraine of any type. Women from these three groups were sent baseline questionnaires on health and lifestyle issues in waves in February 2011 to April 2014. Eligible questionnaire responders were telephone interviewed by physicians, who classified each participant's headaches according to the International Classification of Headache Disorders, 3rd edition beta version (Headache

Classification Committee of the International Headache Society, 2013). Twins with definite migraine with aura and their co-twins were invited to participate. Controls were selected among twin pairs where both twins reported no history of migraine (one twin randomly selected from each pair). Control twins were only included if their non-migraine status was confirmed at interview and if they had less than 30 days of tension-type headache in the preceding year. Detailed eligibility criteria have been presented previously (Gaist et al., 2016). Eligible subjects were invited to participate in the MRI part of the study at a single center in Copenhagen, Denmark. On average, patients were scanned 6 months and controls 4 months after completing the physician-conducted headache interview (Gaist et al., 2016). Detailed information regarding subject recruitment and participation are provided in a previous publication (Gaist et al., 2016). Importantly, analyses comparing participants and non-participants indicated no major selection biases. Subjects received no financial reward for participating. The study was approved by the Ethics Committee of the Region of Southern Denmark and the Danish Data Protection Agency. Written informed consent was obtained from all participants. The study is registered at clinicaltrials.gov (NCT02047695).

### 2.1. MRI acquisition

All participants underwent whole-brain MRI using the same 3.0 T magnetic resonance scanner (Siemens Magnetom Verio, Erlangen, Germany) equipped with a 32-channel receive head coil. Structural imaging was based on a T1-multi-echo 3D FLASH sequence as part of a whole-brain quantitative MRI protocol (Helms and Dechent, 2009) with the following parameters: repetition time = 18.7 ms echo time = 2.20, 4.70, 7.20, 9.70, 12.20 and 14.70 ms, flip, angle 20 degrees, field of view = 256 mm, 176 sagittal slices. In-plane acquisition was accelerated by 2-fold using generalized autocalibrating partially parallel acquisitions (Griswold et al., 2002) with 18 reference lines. Prior to further processing, images with a contrast comparable to standard T1-weighted images were created by averaging across the echoes acquired in the sequence.

T2-weighted images of the whole brain were obtained using a 3D turbo spin echo sequence (repetition time = 3200 ms, echo time = 409 ms, matrix = 256x256, 176 sagittal slices with no gap, 1.0x1.0x1.0 mm<sup>3</sup> isotropic voxels). FLAIR images of the whole brain were obtained using a 3D turbo inversion recovery sequence (repetition time = 5000 ms, echo time = 395 ms, inversion time = 1800 ms, matrix = 256x256, 176 sagittal slices with no gap, 1.0x1.0x1.0 mm<sup>3</sup> isotropic voxels).

### 2.2. Image assessment

All images were assessed by a consultant radiologist (C.G.M.) with experience in neuroradiology who was blinded to headache diagnoses and clinical data. To assess the burden of deep white matter hyperintensities (WMHs), we applied a slightly modified version of Scheltens' semiquantitative scale (Kruit et al., 2004; Scheltens et al., 1993). Periventricular WMHs were assessed in three regions (frontal and posterior horns and bands) and rated as 0 (no periventricular WMH); 1 (pencil-thin lining); 2 (smooth halo or thick lining); or 3 (large confluent lesions). The three regional scores were summed up to a total score (range 0–9). In the present study of thalamic structure, data from subjects with significant deep white matter hyperintensities (Scheltens score 12 or more) or periventricular white matter hyperintensities (Scheltens score 6 or more) were excluded from further analyses.

### 2.3. MRI data analysis

For pre-processing purposes, cortical reconstruction and volumetric segmentation was performed with the FreeSurfer image analysis suite v.6.0.0 (<http://surfer.nmr.mgh.harvard.edu>) using the standard *recon-*

all pipeline. The technical details of these procedures are described in prior publications (Dale et al., 1999; Fischl et al., 1999). In short, reconstruction procedures comprised intensity-normalization to MNI-space, skull-stripping, filtering, segmentation and surface deformation. The quality of the skull-stripping and accuracy of the gray and white matter outer boundaries was reviewed by a trained researcher (S.H.N.) who was blinded to the grouping of the patients. In order to obtain volumetric data of ROIs we used specialised FreeSurfer tools for automated parcellation of gray and white matter (Desikan et al., 2006).

Thalamic nuclei were segmented using two complimentary approaches: 1) the *MAGeT Brain Algorithm* (Chakravarty et al., 2013), a multi-atlas segmentation (MAS) technique previously used in a multi-center migraine study (Magon et al., 2015) and 2) a recently developed algorithm (Iglesias et al., 2018), which relies on a probabilistic atlas derived from ex vivo MRI scans and histological specimens from six post mortem cases (Iglesias et al., 2018).

### 2.3.1. Method 1: MAGeT brain algorithm

Thalamic nuclei were segmented using a multi-agent system (MAS) algorithm that relies on a collection of so-called atlases consisting of MRI scans and corresponding thalamus labelings. In brief, the MAS contains two steps: registration and label fusion. The registration step establishes a spatial correspondence between each atlas and a to-be-segmented target scan. Once a correspondence between each atlas MRI and the target MRI has been established, the labeling is warped to the target space. This procedure results in multiple candidate segmentations, as many as there are atlases, which are then fused into a consensus segmentation in the label fusion step. The technical details of this approach are described in prior publications (Iglesias and Sabuncu, 2015).

The MAGeT algorithm (Chakravarty et al., 2013) is based on a single atlas where the thalamus nuclei labelings were manually drawn on serial histological data. The thalamic nuclei included in the atlas are: Left and right lateral geniculate nucleus, medial geniculate nucleus, anterior nuclei, central nuclei, lateral dorsal, lateral posterior, medial dorsal, pulvinar, ventral anterior nucleus, ventral lateral nucleus and ventral posterior nucleus (see Fig. 1).

We applied our version of the MAGeT algorithm in the following way:

- 1) A non-linear registration of the histological atlas to a subset of 31 subjects (see below) was applied using Advanced Normalization

Tools. The initially segmented subset of subjects was representative with regard to the demographical and clinical features of the sample in order to capture the neuroanatomical variability of the sample. As there was only a single histological atlas, no label fusion was necessary at this step (see Fig. 1).

- 2) Each subject in the representative sample was registered to the remaining subjects in the group ( $31 \times 30$  registrations) in a leave-one-out manner. This resulted in 30 candidate segmentations per subject, which were fused to a consensus segmentation using majority voting where the most frequently occurring label across the candidate labelings was assigned to each voxel (see Fig. 1). The initial segmentations of step 1 can be very noisy as they are based on a single atlas. Thus, we used the leave-one-out cross-registration step to obtain smoother segmentations.
- 3) Finally, the rest of the subjects were segmented using the representative subset of subjects and corresponding segmentations. Each of the 31 atlases were registered to the remaining 255 scans ( $255 \times 31$  registrations) and the candidate segmentations in each subject were obtained using a voxel-wise majority vote. The segmentations were visually inspected to confirm that the outer border of the thalamus matched the intensity gradient in the MR scans by a trained researcher (S.H.N.). Thereby, specific attention was paid to the borders of the thalamus toward cerebrospinal fluid spaces and toward the surrounding white matter.

The representative sample consisted of 31 subjects, 16 healthy controls and 15 patients with migraine with aura. The representative sample, which was chosen from the whole group, was matched for age, disease distribution, number of lifetime aura attacks and number of aura attacks within the last 12 months in order to adequately capture the neuroanatomical variability of the sample. This number of subjects was found optimal to capture the population variability in previous work, and increasing the number did not increase the accuracy of the method (Pipitone et al., 2014).

An overview of the thalamic nuclei included in the atlas is provided in Fig. 2.

### 2.3.2. Method 2: probabilistic atlas of the thalamic nuclei combining ex vivo MRI and histology

The thalamic nuclei were segmented using a fully automated segmentation method freely available as part of the FreeSurfer image analysis suite v.6.0.0. In brief, the segmentation problem is posed in

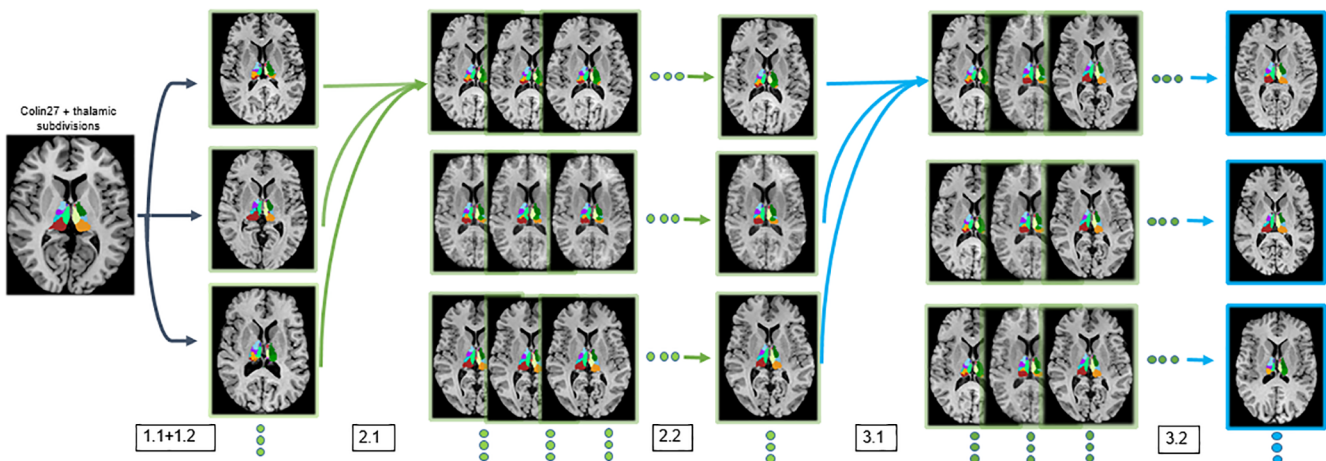


**Fig. 1.** MAGeT Brain Algorithm. This method implies multiple automatically generated registrations from a single histological atlas. Step 1 visualizes the initial step, registration, in the segmentation of the representative sample consisting of 31 subjects using the histological atlas Colin27. This process consists of 1.1) the estimation of a non-linear spatial transformation matching an input template to each subject and 1.2) applying that transformation to each set of labels. In step 2 the initially segmented set of subjects (representative sample) is 2.1) co-registered to each other using a leave-one-out technique and 2.2) the most frequently occurring voxels are chosen using voxelwise majority voting (label fusion). Step 3.1) comprises of the segmentation of the remaining subjects using the majority segmentations of the representative sample. Again, 3.2) the most frequently occurring voxels are chosen using voxelwise majority voting.

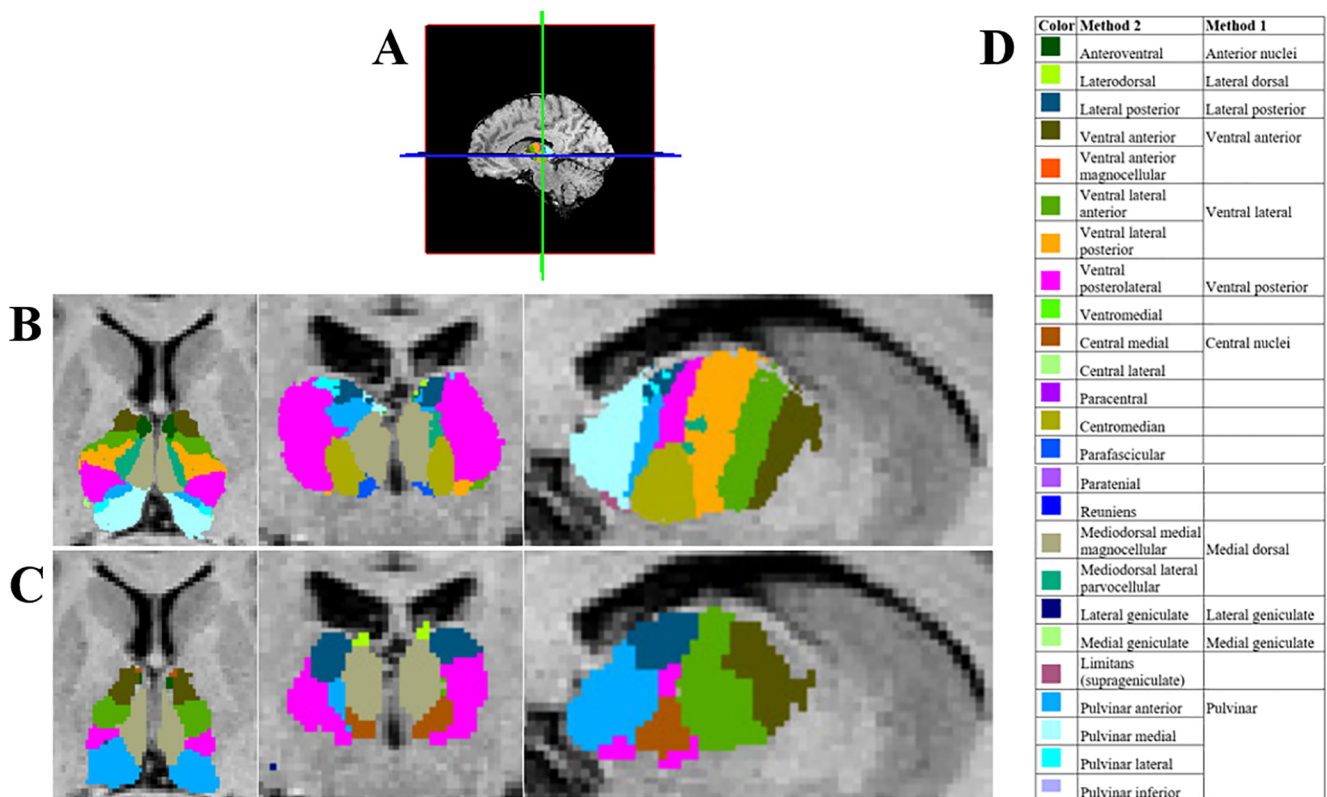


Fig. 2. Representative example from a single subject of the location of thalamic nuclei obtained using segmentation Methods 1 (panel B) and 2 (panel C). Slice locations are shown in panel A, while names of individual nuclei and a colour code is provided in panel D.

terms of Bayesian inference where the task is to find the most probable thalamus nucleus labeling given the MRI scan of a target subject. The registration parameters, along with the parameters of a Gaussian mixture model (GMM) that models the distribution of intensities, are obtained as a maximum-a-posteriori estimate given the data. Subsequently, the segmentation is performed by assigning the most probable nucleus labels to each voxel given the MRI data, and registration and GMM parameters. Details on the segmentation approach can be found in previous publications (Iglesias et al., 2015; Puonti et al., 2016). An overview of the thalamic nuclei included in the atlas is provided in Fig. 2.

#### 2.4. Statistical analyses

All analyses comparing volumes of regions of interest between groups were performed using R statistical software v3.5.2 and the 'nlme' package v3.1.

We hypothesized a priori that, on a group level, thalamic nuclei volumes of both hemispheres would differ relative to corresponding volumes of controls. Theoretically, in the individual migraine patient, abnormal thalamic nuclei volumes could depend on the laterality of the perceived symptoms, e.g. patients predominantly experiencing right-sided pain or right-sided visual symptoms could have structural alterations of the left thalamus. However, clinical information relating to symptom laterality was not available in the present study. For these reasons, we compared left–right averages of thalamic volumes between groups rather than comparing left-sided and right-sided nuclei specifically

##### 2.4.1. Individual-based analyses

The volumes of the thalamic nuclei (11 bilateral nuclei in Method 1 and 25 bilateral nuclei in Method 2) of patients were compared with the volume of the thalamic nuclei of controls in a linear mixed model with

fixed effects covariates (age, educational level (low, medium, high), BMI, smoking, alcohol (units per week) and hypertension (blood pressure of > 160 systolic, or > 95 diastolic, or current use of anti-hypertensive drugs)) and random intercepts. The fixed covariates were included in the final model if significant at a probability level of less than 0.05 estimated by likelihood ratio testing (using forward stepwise selection). An interaction term between the subject category (i.e. patient or control) variable and the regions of interest (thalamic nuclei) was included to test if patients and controls differed in volume of the thalamic nuclei considering all differences at the remaining regions. The dependence of the different regions within individuals was captured by a random intercept. Since confounding due to any between-group differences in the volume of the whole thalamus would be avoided using this approach, we did not normalize the volumes of the thalamic nuclei to head size or intracranial volume. A separate intercept captured dependency of individuals where both twins in a pair were included (18 pairs where both twins had migraine with aura were included). Inference on the difference in volume and the corresponding 95% confidence intervals (CIs) were obtained for each location in the model using Wald tests of the relevant contrast, and a two-sided probability level of less than 0.05 was considered statistically significant. Within each of the two methods the results were corrected for testing of multiple thalamic nuclei using the Benjamini-Hochberg False Discovery Rate (FDR) approach set at an  $\alpha$  level of 0.05.

Further, we investigated whether there was a relation between migraine aura frequency (categorical data of aura attacks during the last 12 months and lifetime number of aura attacks, respectively, see Table 1) and the volumes of thalamic nuclei. This was done using two additional linear mixed models that were applied to the patient data specifically: one including an interaction term between aura attacks in the past 12 months and the thalamic nuclei volumes, and one including an interaction term between lifetime number of aura attacks and the thalamic nuclei volumes. These models included the same fixed effects



**Table 1**  
Characteristics of study participants.

Characteristic	Individual-based analyses			Within-pair analyses		
	Patients with migraine with aura n = 156	Controls n = 126	P value <sup>a</sup>	Patients with migraine with aura n = 29	Co-twins n = 29	P value <sup>b</sup>
Age at time of MRI scan, years	47.5 ± 6.4	47.4 ± 7.6	0.69	49.4 ± 5.2	49.5 ± 5.2	0.33
Zygoty – no. (%)						
Monozygotic	68 (43.6)	50 (39.7)	0.53	14	14	1.00
Dizygotic – same sex	57 (36.5)	48 (38.1)	0.80	15	15	1.00
Dizygotic – opposite sex	31 (19.9)	28 (22.2)	0.64	NA	NA	NA
Low education level <sup>c</sup> – no. (%)	50 (32.1)	32 (25.4)	0.22	6 (20.7)	9 (31.0)	0.18
Smoker, ever – no. (%)	79 (50.6)	62 (49.2)	0.78	15 (51.7)	14 (48.3)	1.00
Alcohol, drinks per week	3.7 ± 5.2	4.8 ± 5.4	0.07	3.5 ± 2.9	3.7 ± 3.7	0.71
BMI <sup>d</sup>	24.8 ± 4.3	24.6 ± 4.3	0.72	25.1 ± 4.0	24.5 ± 3.5	0.33
Hypertension <sup>e</sup> – no. (%)	49 (31.4)	26 (20.6)	0.048	12 (40.0)	11 (36.7)	0.75
Scheltens scores <sup>f</sup>						
Periventricular white matter hyperintensities	3 ± 2	2 ± 2	0.75	1 ± 1	2 ± 2	0.40
Deep white matter hyperintensities	1 ± 3	1 ± 3	0.85	2 ± 4	2 ± 5	0.40
Migraine with aura						
Age at onset, years	23.0 (10.9)	NA		25.4 (10.6)	NA	
Age at last attack <sup>g</sup> , years	42.6 (9.7)	NA		41.5 (11.3)	NA	
Aura attacks in last 12 months <sup>g,h</sup> – no. (%)						
0	57 (36.5)	NA		18 (62.1)	NA	
1–5	69 (44.2)	NA		9 (31.0)	NA	
> 5	29 (18.6)	NA		2 (6.9)	NA	
Headache presence in relation to aura – no. (%)						
Always aura with headache	97 (62.2)	NA		19 (65.5)	NA	
Aura with & without headache	47 (30.1)	NA		9 (31.0)	NA	
Aura never with headache	12 (7.7)	NA		1 (3.5)	NA	
Aura type – no. (%)						
Visual	154 (98.7)	NA		28 (96.6)	NA	
Sensory	32 (20.5)	NA		3 (10.3)	NA	
Aphasia	18 (11.5)	NA		4 (13.8)	NA	
Motor	1 (0.6)	NA		1 (3.5)	NA	
Lifetime no. of aura attacks – no. (%)						
2–9	35 (22.4)	NA		10 (34.5)	NA	
10–49	47 (30.1)	NA		12 (41.4)	NA	
50–100	31 (19.9)	NA		4 (13.8)	NA	
> 100	43 (27.6)	NA		3 (10.3)	NA	
Migraine without aura						
Ever <sup>i</sup> – no. (%)	33 (21.2)	NA		8 (27.6)	10 (34.5)	0.44
Lifetime no. of attacks – no. (%)						
5–49	7 (4.5)	NA		1 (3.5)	5 (17.2)	
50–100	9 (5.8)	NA		5 (17.2)	1 (3.5)	
> 100	17 (10.9)	NA		2 (6.9)	4 (13.8)	0.44
Last 12 months <sup>g</sup> , no. of attacks – no. (%)						
0	13 (8.3)	NA		5 (17.2)	2 (6.9)	
1–5	17 (10.9)	NA		2 (6.9)	4 (13.8)	
≥ 6	8 (5.1)	NA		1 (3.5)	4 (13.8)	0.08
Days with tension-type headache in last 12 months <sup>g</sup> – no. (%)						
0–13	112 (71.8)	117 (92.9)		25 (86.2)	24 (82.8)	
14–30	26 (16.7)	9 (7.1)		3 (10.3)	4 (13.8)	
31–179 <sup>j</sup>	18 (11.5)	0	0.33	1 (3.4)	1 (3.5)	0.71
Headache in 48 h before or 48 h after study scan <sup>k</sup> – no. (%)						
Any type of headache	29 (18.6)	7 (5.6)	0.51	5 (17.2)	8 (27.6)	0.35
Migraine <sup>l</sup>	3 (1.9)	0	NA	0	2 (6.9)	NA

Means ± standard deviation, unless otherwise specified.

<sup>a</sup> Patients versus controls. Generalized linear mixed models (binomial for proportions and Gaussian for means) were used to test the null hypothesis: there is no difference between patients and controls. Random intercepts for twin pairs were included to adjust for twin pair cluster effects.

<sup>b</sup> Patients versus co-twins. Generalized linear mixed models (binomial for proportions and Gaussian for means) were used to test the null hypothesis: there is no difference between patients and co-twins. Random intercepts for twin pairs were included to adjust for twin pair status.

<sup>c</sup> Education level was defined as low in women with less than 12 years of schooling and less than 3 years of vocational training.

<sup>d</sup> Body Mass Index, the weight in kg divided by the square of the height in meters.

<sup>e</sup> Hypertension was defined as systolic blood pressure of 160 mmHg or higher, or diastolic blood pressure of 95 mmHg or higher, or current use of antihypertensive drugs for hypertension.

<sup>f</sup> Values for Scheltens scores are medians ± interquartile range

<sup>g</sup> In 12 months before physician-conducted phone interview, establishing headache diagnoses according to International Headache Society classification criteria.

<sup>h</sup> Information missing for 1 patient.

<sup>i</sup> Per protocol, co-twins with migraine without aura could be included in the study.

<sup>j</sup> Potential controls with > 30 tension-type headache days in 12 months prior to interview were excluded by design.

<sup>k</sup> Participants completed questionnaire information on headaches within last 48 h on the day they were scanned and were subsequently phone-interviewed by a physician 48–72 h after the scan to verify this information and to ascertain presence of headaches during or after the study scan.

<sup>l</sup> Participants reported exclusively migraine without aura attacks.

covariates and intercepts as described above. We used likelihood ratio testing to determine if inclusion of the migraine aura frequency covariates provided a better fit compared to similar models without these covariates. Further, we created boxplots for each thalamic nucleus showing the volume distribution in the different migraine aura frequency groups (aura attacks during the last 12 months and lifetime number of aura attacks plotted separately, see [Supplementary Figs. 1–4](#)).

#### 2.4.2. Within-pair analyses

In the within-pair analysis, we investigated intrapair differences in mean volumes of the thalamic nuclei of twin pairs, where one of the twins had migraine with aura and the co-twin did not suffer from migraine with aura. This was done using paired t-tests, since this matched-pair analysis reduces the influence of several unmeasured confounders, and thus relies on the assumption of discordance in exposure and outcome. We abstained from within-pair analyses stratified by zygosity due to the small number of discordant twin pairs (14 monozygotic and 15 dizygotic pairs) that participated in the study. Results were corrected for testing of multiple thalamic nuclei using the Benjamini-Hochberg False Discovery Rate (FDR) approach set at an  $\alpha$  level of 0.05.

### 3. Results

A total of 172 migraine patients with aura, 34 co-twins and 139 controls were scanned. Due to imaging quality issues, 6 scans from patients, 4 scans from co-twins, and 2 scans from controls were excluded. In addition, 10 patients and 11 controls were excluded because they exceeded the a priori defined level of acceptable WMH burden. Thus, the results are based on data from 156 patients, 29 co-twins, and 126 controls. Patients were similar to controls with regard to age, and several lifestyle characteristics, although 31.4% of patients were classified as hypertensive, compared with 20.6% of controls ( $P = 0.048$ ) ([Table 1](#)). Headache characteristics of patients corresponded to our expectations based on previous population-based epidemiological studies of migraine with aura ([Eriksen et al., 2004](#); [Russell and Olesen, 1996](#)).

#### 3.1. Patients compared to controls

The inclusion of the fixed effects covariates in the full model (age, educational level, BMI, smoking, alcohol, and hypertension) produced similar results, but a better fit than more parsimonious models (likelihood ratio testing  $P < 0.05$ ). This was the case for results from both Method 1 and Method 2.

According to the best fitted (i.e. full) model, we found no statistically significant volume differences of the thalamic nuclei using Method 1 or Method 2 after correction for multiple comparisons (see [Tables 2 and 3](#)). Results corrected only for the effects of age are presented in [Supplementary Tables 1 and 2](#).

Within the patient group we did not find any indications of the thalamic nuclei volumes being dependent on the number of migraine aura attacks during the past 12 months or lifetime number of aura attacks (see [Supplementary Figs. 1–4](#)).

#### 3.2. Patients compared to co-twins

The within-pair analyses showed no volume differences for any nuclei between patients and co-twins. This was the case for Method 1 and Method 2 (see [Tables 4 and 5](#)).

### 4. Discussion

In this large, population-based study of a well-characterized sample of migraine patients with aura, compared to matched healthy controls and to aura-free co-twins, using two complementary, advanced analysis methods, we did not find any between-group differences of thalamic nuclei volumes. Further, we did not find a relation between migraine aura frequency and thalamic nuclei volumes in this dataset.

#### 4.1. Previous studies of thalamic nuclei volumes in migraine

A previous, multi-centre study of 131 migraine patients (38 with aura, mean age 30.8 years, 109 women, mean monthly attack frequency 3.2, mean disease duration 14 years) recruited from four international tertiary headache centres reported smaller volumes in patients of the central nuclear complex, anterior nucleus, and lateral dorsal nucleus, compared to 115 healthy volunteers. The study used 3D T1-weighted MR images acquired at 3 T and the MAgE Brain Algorithm, corresponding to “Method 1” of the present study. The study found no between-group differences in separate analyses of controls vs. migraine patients without aura, controls vs. migraine patients with aura, and patients with aura vs. patients without aura. Another previous 3 T MRI study compared thalamic nuclei volumes of 35 migraine without aura patients (mean age 37.9 years, 26 women, mean monthly attack frequency 3.8, mean disease duration 9.2 years) from a single South Korean tertiary centre to those of 40 healthy volunteers using a probabilistic atlas-based approach identical to “Method 2” of the present study. This study reported larger volumes in the patient group of the medial geniculate and anteroventral nuclei and smaller volumes of the parafascicular nuclei. In summary, the two previous studies had the same objective of evaluating volumes of thalamic nuclei in migraine patients, used comparable input data, applied two different data analysis methods, and reached different conclusions. The most important differences between the two previous studies and the present study are that 1) we included only women and only migraine patients *with* aura, 2) patients of the present study had a markedly lower attack frequency, 3) patients of the previous studies were recruited from specialized headache centres and may not be comparable to migraine patients of the general population.

**Table 2**

Results from Method 1. Volumes of thalamic nuclei in 156 women with migraine with aura compared with 126 migraine-free women. Values of volumes are in  $\text{mm}^3$  (SD).

Structure	Patients with migraine with aura	Controls	P value <sup>1</sup>
Anterior nuclei	205.47 (29.99)	209.08 (32.91)	0.98
Central nuclei	421.19 (37.51)	422.61 (43.18)	0.98
Lateral dorsal	45.69 (11.58)	47 (12.37)	0.98
Lateral geniculate nucleus	310.16 (40.46)	309.1 (45.76)	0.98
Lateral posterior	648.99 (80.8)	664.36 (94.38)	0.98
Medial dorsal	1732.42 (190.04)	1711.85 (180.64)	0.98
Medial geniculate nucleus	301.33 (26.24)	298.83 (32.61)	0.98
Pulvinar	2996.72 (275.48)	2956.33 (312.38)	0.11
Ventral anterior nucleus	937.36 (114.15)	951.57 (139.54)	0.98
Ventral lateral nucleus	1375.38 (141.64)	1397.63 (177.19)	0.98
Ventral posterior nucleus	903.81 (82.62)	908.02 (105.43)	0.98

<sup>1</sup> P values are corrected for comparison of multiple nuclei using the Benjamini-Hochberg False Discovery Rate (FDR) approach.

**Table 3**

Results from Method 2. Volumes of thalamic nuclei in 156 women with migraine with aura compared with 126 migraine-free women. Values of volumes are in mm<sup>3</sup> (SD).

Structure	Patients with migraine with aura	Controls	P value <sup>1</sup>
Anteroventral	259.51 (33.06)	259.77 (32.09)	0.96
Central medial	142.05 (18.49)	141.82 (17.13)	0.96
Central lateral	81.98 (12.86)	79.91 (11.67)	0.96
Centromedian	514.09 (48.51)	509.21 (57.96)	0.96
Limits supragenulate	54.08 (9.87)	51.65 (9.84)	0.96
Laterodorsal	63.54 (13.09)	61.57 (12.81)	0.96
Lateral geniculate	273.21 (52.63)	269.14 (46.26)	0.96
Lateroposterior	253.88 (27.47)	253.5 (31.25)	0.96
Mediodorsal lateral parvocellular	599.16 (76.02)	591.85 (66.8)	0.96
Mediodorsal medial magnocellular	1469.43 (177.27)	1466.37 (146.37)	0.96
Medial geniculate	211.08 (31.13)	207.68 (27.27)	0.96
Medial ventral reuniens	28.65 (4.07)	28.19 (3.86)	0.96
Paracentral	6.43 (0.93)	6.54 (0.84)	0.96
Parafascicular	123.19 (12.12)	123.02 (14.61)	0.96
Paratentorial	13.77 (1.36)	13.62 (1.56)	0.96
Pulvinar anterior	363.63 (47.93)	357.21 (40.12)	0.96
Pulvinar inferior	297.24 (43.7)	293.81 (43.05)	0.96
Pulvinar lateral	314.31 (45.15)	311.19 (43.8)	0.96
Pulvinar medial	1665.79 (180.88)	1643.33 (175.53)	0.96
Ventral anterior	756.31 (86.52)	763.21 (83.5)	0.96
Ventral anterior magnocellular	65.29 (7.06)	65.5 (6.23)	0.96
Ventral lateral anterior	1191.62 (128.84)	1207.21 (139.05)	0.96
Ventral lateral posterior	1574.31 (161.52)	1587.56 (180.1)	0.96
Ventromedial	38.93 (4.67)	38.45 (4.79)	0.96
Ventral posterolateral	1588.31 (172.94)	1577.88 (180.24)	0.96
Whole thalamus	11949.78 (1086.98)	11909.18 (1053.51)	0.96

<sup>1</sup> P values are corrected for comparison of multiple nuclei using the Benjamini-Hochberg False Discovery Rate (FDR) approach.

**Table 4**

Results from Method 1. Volumes of thalamic nuclei in 29 women with migraine with aura and their twin sisters with no history of migraine with aura. Values of volumes are in mm<sup>3</sup> (SD).

Structure	Patients	Controls	P value <sup>1</sup>
Anterior nuclei	198.31 (28.2)	195.79 (29.57)	0.95
Central nuclei	418.00 (35.18)	420.1 (40.53)	0.95
Lateral dorsal	45.03 (10.06)	42.41 (11.91)	0.95
Lateral geniculate nucleus	298.52 (37.03)	308.24 (38.83)	0.95
Lateral posterior	654.07 (79.18)	610.72 (76.14)	0.44
Medial dorsal	1752.07 (190.31)	1755.03 (185.97)	0.95
Medial geniculate nucleus	309.83 (28.04)	310.66 (26.12)	0.95
Pulvinar	2978.83 (286.45)	3026.52 (289.88)	0.95
Ventral anterior nucleus	936.14 (134.28)	913 (118.29)	0.95
Ventral lateral nucleus	1396.76 (191.18)	1370.14 (154.03)	0.95
Ventral posterior nucleus	910.72 (109.97)	902.55 (98.75)	0.95

<sup>1</sup> P values are corrected for comparison of multiple nuclei using the Benjamini-Hochberg False Discovery Rate (FDR) approach.

While our results indicate no abnormalities of thalamic volume in migraine patients with aura in general, we cannot rule out that such abnormalities might be present in migraine patients without aura specifically, or more severely affected migraine patients. Indeed, alteration of thalamic structure could be a consequence of repeated migraine headache attacks. A correlation between migraine attack frequency or disease duration and the volumes of thalamic nuclei would support the latter possibility. However, none of the two previous studies, or the present study, found such correlations.

**Table 5**

Results from Method 2. Volumes of thalamic nuclei in 29 women with migraine with aura and their twin sisters with no history of migraine with aura. Values of volumes are in mm<sup>3</sup> (SD).

Structure	Patients	Controls	P value <sup>1</sup>
Anteroventral	256.3 (41.12)	257.1 (34.91)	0.99
Central medial	142.05 (18.95)	142.52 (22.09)	0.99
Central lateral	81.31 (13.14)	85.35 (14.85)	0.99
Centromedian	513.14 (68.56)	512.05 (49.82)	0.99
Limits supragenulate	62.04 (13.46)	68.01 (13.46)	0.99
Laterodorsal	256.27 (44.25)	259.63 (55.02)	0.99
Lateral geniculate	246.08 (33.93)	253.14 (33.11)	0.99
Lateroposterior	54.37 (10.38)	54.15 (9.01)	0.99
Mediodorsal lateral parvocellular	597.72 (88.68)	592.06 (75.18)	0.99
Mediodorsal medial magnocellular	1489.23 (193.77)	1469.5 (176.02)	0.99
Medial geniculate	205.39 (28.78)	207.5 (30.13)	0.99
Medial ventral reuniens	28.71 (3.87)	29.11 (5.05)	0.99
Paracentral	6.4 (0.8)	6.41 (0.85)	0.99
Parafascicular	119.94 (14.16)	122.17 (11.33)	0.99
Paratentorial	13.76 (1.77)	13.82 (1.5)	0.99
Pulvinar anterior	354.37 (44.26)	353.92 (40.72)	0.99
Pulvinar inferior	280.98 (44.89)	290.86 (38.9)	0.99
Pulvinar lateral	307.44 (54.55)	297.58 (40.43)	0.99
Pulvinar medial	1635.42 (200.34)	1659.4 (176.85)	0.99
Ventral anterior	752.67 (103.67)	751.7 (91.19)	0.99
Ventral anterior magnocellular	64.73 (7.64)	64.91 (6.85)	0.99
Ventral lateral anterior	1181.05 (157.14)	1174 (117.53)	0.99
Ventral lateral posterior	1558.95 (206.5)	1545.34 (147.58)	0.99
Ventromedial	38.71 (5.52)	38.25 (4.56)	0.99
Ventral posterolateral	1574.9 (215.74)	1554.61 (167.1)	0.99
Whole thalamus	11821.93 (1365.34)	11803.09 (1070.5)	0.99

<sup>1</sup> P values are corrected for comparison of multiple nuclei using the Benjamini-Hochberg False Discovery Rate (FDR) approach.

#### 4.2. Other studies of thalamic structure in migraine

A large (N = 918 total, 143 migraine patients) population-based study using surface-based morphometry to investigate subcortical grey matter structure volumes in headache sufferers, including migraine patients, found no abnormalities of the volume of thalamus related to migraine or other headache types (Husøy et al., 2018). In support, a clinic-based study comparing thalamic volume of 60 patients with migraine with aura (42 women, 18 men) to age and gender matched healthy controls, found no difference between groups (Hougaard et al., 2016). Several studies have used voxel-based morphometry (VBM) to look for differences in grey matter volume between migraine patients and controls with inconsistent results (Hougaard et al., 2014). Interestingly in this context, VBM abnormalities of the thalamus related to migraine have not been reported (Hu et al., 2015).

A combination of different MRI contrasts, quantitative T1, magnetization transfer ratio (MTR), quantitative T2\*, and generalised fractional anisotropy, was used in a study to explore thalamic microstructure in migraine patients with and without aura (Granziera et al., 2014). The authors of this study reported shorter thalamic T1 relaxation time and higher MTR and T2\* relaxation time specifically in migraine with aura and speculated that these changes could represent increased iron deposition and myelin content/cellularity in the thalamus as a whole. The authors further concluded that these differences were not related to pain processing, since the ventral-postero-medial and ventral-postero-lateral nuclei were not specifically affected. Indeed, a recent fMRI study of pain processing in interictal migraine with aura did not find abnormal thalamic activation (Russo et al., 2019).

### 4.3. Strengths and limitations of the present study

A main strength of the present study was the use of the population-based Danish Twin Registry, which enabled us to identify a large number of well-characterised patients and matched controls. Rather than studying a mixed migraine population (migraine without aura and migraine with aura patients), the present study specifically focused on a pure phenotype of migraine patients with aura. Also, we were able to perform paired analyses of twin pairs discordant for migraine with aura, an approach that strongly reduced or eliminated potential confounding effects of genes and common environment. The migraine diagnosis was established through telephone interviews with physicians based on internationally acknowledged criteria and all subjects were scanned using the same MRI scanner at a single centre. Some potential limitations also need to be considered. A subgroup (36.5%) of patients had not had a migraine attack in the previous year. Thus, we may have been unable to detect potential structural thalamic abnormalities related to frequent or recent migraine attacks. The paired analyses were based on 29 cases compared to 29 controls and thus probably only had power to detect relatively large differences in thalamic nuclei volume. We cannot rule out that small between-group differences would have been detectable in a larger sample size. Our results obtained in women do not generalise to male patients. Indeed, previous MRI studies showed differences in thalamic volume and thalamic microstructure between men and women (Lotze et al., 2019; Menzler et al., 2011), although with conflicting results (Ruigrok et al., 2014). Due to the observational nature of this study, it we cannot rule out the possibility that unmeasured or insufficiently measured confounders may have influenced our results.

Based on the results of the present study, we cannot exclude potential microstructural abnormalities or abnormal thalamic function in migraine with aura.

In conclusion, our results indicate that female migraine patients with aura do not have abnormal volumes of thalamic nuclei.

### CRediT authorship contribution statement

**Anders Hougaard:** Conceptualization, Formal analysis, Writing - original draft. **Silas Haahr Nielsen:** Methodology, Formal analysis, Writing - original draft. **David Gaist:** Conceptualization, Formal analysis, Project administration, Funding acquisition, Writing - review & editing. **Oula Puonti:** Methodology, Formal analysis, Writing - review & editing. **Ellen Garde:** Formal analysis, Writing - review & editing. **Nina Linde Reislev:** Investigation, Writing - review & editing. **Pernille Iversen:** Investigation, Writing - review & editing. **Camilla Gøbel Madsen:** Investigation, Writing - review & editing. **Morten Blaabjerg:** Investigation, Writing - review & editing. **Helle Hvilsted Nielsen:** Investigation, Writing - review & editing. **Thomas Krøigård:** Investigation, Writing - review & editing. **Kamilla Østergaard:** Investigation, Writing - review & editing. **Kirsten Ohm Kyvik:** Investigation, Writing - review & editing. **Kristoffer Hougaard Madsen:** Conceptualization, Formal analysis, Writing - review & editing. **Hartwig Roman Siebner:** Supervision, Project administration, Funding acquisition, Writing - review & editing. **Messoud Ashina:** Supervision, Project administration, Funding acquisition, Writing - review & editing.

### Acknowledgements

The study received support from the Lundbeck Foundation (R93-A8392), Novo Nordisk Foundation and Fabrikant Vilhelm Pedersen and Hustrus legat, Fonden til Lægevidenskabens Fremme, and A.P. Møller og Hustru Chastine Mc-Kinney Møllers Fond til Almene Formaal. D.G. is funded by Odense University Hospital. M.A. is funded by Novo Nordisk Foundation (1014333).

### Conflicts of interest

H.R.S. has received honoraria as speaker from Sanofi Genzyme, Denmark and Novartis, Denmark, as consultant from Sanofi Genzyme, Denmark and as senior editor (NeuroImage) and Editor in Chief (NeuroImage: Clinical) from Elsevier Publishers, Amsterdam, The Netherlands. He has received royalties as book editor from Springer Publishers, Stuttgart, Germany.

M.A. is a consultant, speaker or scientific advisor for Alder, Allergan, Amgen, Alder, Eli Lilly, Lundbeck, Novartis, and Teva, primary investigator for Alder, Allergan, Amgen, Eli Lilly, Novartis and Teva trials. MA reports research grants from Lundbeck Foundation, Novo Nordisk Foundation and Novartis. MA has no ownership interest and does not own stocks of any pharmaceutical company. MA serves as associate editor of Cephalalgia, associate editor of Headache, co-editor of the Journal of Headache and Pain. MA is President of the International Headache Society.

A.H. has received honoraria for lecturing from Allergan, Novartis, and Teva and serves on the scientific advisory board of BalancAir inc.

The remaining authors declare no conflicts of interest.

### Appendix A. Supplementary data

Supplementary data to this article can be found online at <https://doi.org/10.1016/j.nicl.2020.102361>.

### References

- Burstein, R., Jakubowski, M., Garcia-Nicas, E., Kainz, V., Bajwa, Z., Hargreaves, R., Becerra, L., Borsook, D., 2010. Thalamic sensitization transforms localized pain into widespread allodynia. *Ann. Neurol.* 68, 81–91. <https://doi.org/10.1002/ana.21994>.
- Chakravarty, M.M., Steadman, P., van Eede, M.C., Calcott, R.D., Gu, V., Shaw, P., Raznahan, A., Collins, D.L., Lerch, J.P., 2013. Performing label-fusion-based segmentation using multiple automatically generated templates. *Hum. Brain Mapp.* 34, 2635–2654. <https://doi.org/10.1002/hbm.22092>.
- Charles, A., Hansen, J.M., 2015. Migraine aura. *Curr. Opin. Neurol.* 28, 255–260. <https://doi.org/10.1097/WCO.0000000000000193>.
- Dale, A.M., Fischl, B., Sereno, M.I., 1999. Cortical surface-based analysis. I. Segmentation and surface reconstruction. *Neuroimage* 9, 179–194. <https://doi.org/10.1006/nimg.1998.0395>.
- de Tommaso, M., Ambrosini, A., Brighina, F., Coppola, G., Perrotta, A., Pierelli, F., Sandrini, G., Valeriani, M., Marinazzo, D., Stramaglia, S., Schoenen, J., 2014. Altered processing of sensory stimuli in patients with migraine. *Nat. Rev. Neurol.* 10, 144–155. <https://doi.org/10.1038/nrneuro.2014.14>.
- Desikan, R.S., Ségonne, F., Fischl, B., Quinn, B.T., Dickerson, B.C., Blacker, D., Buckner, R.L., Dale, A.M., Maguire, R.P., Hyman, B.T., Albert, M.S., Killiany, R.J., 2006. An automated labeling system for subdividing the human cerebral cortex on MRI scans into gyral based regions of interest. *Neuroimage* 31, 968–980. <https://doi.org/10.1016/j.neuroimage.2006.01.021>.
- Eriksen, M., Thomsen, L., Andersen, I., Nazim, F., JJ, O., 2004. Clinical characteristics of 362 patients with familial migraine with aura. *Cephalalgia* 24, 564–575, doi: 10.1111/j.1468-2982.2003.00718.x.
- Fischl, B., Sereno, M.I., Dale, A.M., 1999. Cortical surface-based analysis. II: Inflation, flattening, and a surface-based coordinate system. *Neuroimage* 9, 195–207. <https://doi.org/10.1006/nimg.1998.0396>.
- Gaist, D., Garde, E., Blaabjerg, M., Nielsen, H.H., Krøigård, T., Østergaard, K., Møller, H.S., Hjelmberg, J., Madsen, C.G., Iversen, P., Kyvik, K.O., Siebner, H.R., Ashina, M., 2016. Migraine with aura and risk of silent brain infarcts and white matter hyperintensities: an MRI study. *Brain* 139, 2015–2023. <https://doi.org/10.1046/j.1526-4610.1999.3903173.x>.
- Gaist, D., Hougaard, A., Garde, E., Reislev, N.L., Wiwie, R., Iversen, P., Madsen, C.G., Blaabjerg, M., Nielsen, H.H., Krøigård, T., Østergaard, K., Kyvik, K.O., Hjelmberg, J., Madsen, K., Siebner, H.R., Ashina, M., 2018. Migraine with visual aura associated with thicker visual cortex. *Brain* 141, 776–785. <https://doi.org/10.1093/brain/awx382>.
- Gaist, D., Pedersen, L., Madsen, C., Tsiropoulos, I., Bak, S., Sindrup, S., McGue, M., Rasmussen, B.K., Christensen, K., 2005. Long-term effects of migraine on cognitive function: a population-based study of Danish twins. *Neurology* 64, 600–607. <https://doi.org/10.1212/01.WNL.0000151858.15482.66>.
- Granziera, C., Daducci, A., Romascano, D., Roche, A., Helms, G., Krueger, G., Hadjikhani, N., 2014. Structural abnormalities in the thalamus of migraineurs with aura: a multiparametric study at 3 T. *Hum. Brain Mapp.* 35, 1461–1468. <https://doi.org/10.1002/hbm.22266>.
- Griswold, M.A., Jakob, P.M., Heidemann, R.M., Nittka, M., Jellus, V., Wang, J., Kiefer, B., Haase, A., 2002. Generalized autocalibrating partially parallel acquisitions (GRAPPA). *Magn. Reson. Med.* 47, 1202–1210. <https://doi.org/10.1002/mrm.10171>.



- Headache Classification Committee of the International Headache Society, 2018. The International Classification of Headache Disorders, third ed. Cephalalgia 38, 1–211, doi: 10.1177/0333102417738202.
- Headache Classification Committee of the International Headache Society, 2013. The International Classification of Headache Disorders, third ed. (beta version). Cephalalgia 33, 629–808, doi:10.1177/0333102413485658.
- Helms, G., Dechent, P., 2009. Increased SNR and reduced distortions by averaging multiple gradient echo signals in 3D FLASH imaging of the human brain at 3T. J. Magn. Reson. Imaging 29, 198–204. <https://doi.org/10.1002/jmri.21629>.
- Hougaard, A., Amin, F.M., Arnglim, N., Vlachou, M., Larsen, V.A., Larsson, H.B.W., Ashina, M., 2016. Sensory migraine aura is not associated with structural grey matter abnormalities. YNICL 11, 322–327. <https://doi.org/10.1016/j.nicl.2016.02.007>.
- Hougaard, A., Amin, F.M., Ashina, M., 2014. Migraine and structural abnormalities in the brain. Curr. Opin. Neurol. 27, 309–314. <https://doi.org/10.1097/WCO.000000000000086>.
- Hu, W., Guo, J., Chen, N., Guo, J., He, L., 2015. A meta-analysis of voxel-based morphometric studies on migraine. Int. J. Clin. Exp. Med. 8, 4311–4319.
- Husøy, A.K., Pintzka, C., Eikenes, L., Håberg, A.K., Hagen, K., Linde, M., Stovner, L.J., 2018. Volume and shape of subcortical grey matter structures related to headache: a cross-sectional population-based imaging study in the Nord-Trøndelag Health Study. Cephalalgia 39, 173–184. <https://doi.org/10.1016/j.pmrj.2013.03.004>.
- Iglesias, J.E., Augustinack, J.C., Nguyen, K., Player, C.M., Player, A., Wright, M., Roy, N., Frosch, M.P., McKee, A.C., Wald, L.L., Fischl, B., Van Leemput, K., Initiative, Alzheimer's Disease Neuroimaging, 2015. A computational atlas of the hippocampal formation using ex vivo, ultra-high resolution MRI: application to adaptive segmentation of in vivo MRI. Neuroimage 115, 117–137. <https://doi.org/10.1016/j.neuroimage.2015.04.042>.
- Iglesias, J.E., Insausti, R., Lerma-Usabiaga, G., Bocchetta, M., Van Leemput, K., Greve, D.N., van der Kouwe, A., Initiative, Alzheimer's Disease Neuroimaging, Fischl, B., Caballero-Gaudes, C., Paz-Alonso, P.M., 2018. A probabilistic atlas of the human thalamic nuclei combining ex vivo MRI and histology. Neuroimage 183, 314–326. <https://doi.org/10.1016/j.neuroimage.2018.08.012>.
- Iglesias, J.E., Sabuncu, M.R., 2015. Multi-atlas segmentation of biomedical images: a survey. Med. Image Anal. 24, 205–219. <https://doi.org/10.1016/j.media.2015.06.012>.
- Kruit, M.C., van Buchem, M.A., Hofman, P.A.M., Bakkers, J.T.N., Terwindt, G.M., Ferrari, M.D., et al., 2004. Migraine as a risk factor for subclinical brain lesions. JAMA 291, 427–434.
- Lotze, M., Domin, M., Gerlach, F.H., Gaser, C., Lueders, E., Schmidt, C.O., Neumann, N., 2019. Novel findings from 2,838 AdultBrains on Sex Differences in GrayMatter Brain Volume. Sci. Rep. 1–7. <https://doi.org/10.1038/s41598-018-38239-2>.
- Magon, S., May, A., Stankewitz, A., Goadsby, P.J., Tso, A.R., Ashina, M., Amin, F.M., Seifert, C.L., Chakravarty, M.M., Müller, J., Sprenger, T., 2015. Morphological Abnormalities of Thalamic Subnuclei in Migraine: A Multicenter MRI Study at 3 Tesla. J. Neurosci. 35, 13800–13806. <https://doi.org/10.1523/JNEUROSCI.2154-15.2015>.
- Menzler, K., Belke, M., Wehrmann, E., Krakow, K., Lengler, U., Jansen, A., Hamer, H.M., Oertel, W.H., Rosenow, F., Knake, S., 2011. Men and women are different: Diffusion tensor imaging reveals sexual dimorphism in the microstructure of the thalamus, corpus callosum and cingulum. Neuroimage 54, 2557–2562. <https://doi.org/10.1016/j.neuroimage.2010.11.029>.
- Nosedà, R., Bernstein, C.A., Nir, R.-R., Lee, A.J., Fulton, A.B., Bertisch, S.M., Hovaguimian, A., Cestari, D.M., Saavedra-Walker, R., Borsook, D., Doran, B.L., Buettner, C., Burstein, R., 2016. Migraine photophobia originating in cone-driven retinal pathways. Brain aww119. <https://doi.org/10.1093/brain/aww119>.
- Pipitone, J., Park, M.T.M., Winterburn, J., Lett, T.A., Lerch, J.P., Pruessner, J.C., Lepage, M., Voineskos, A.N., Chakravarty, M.M., Alzheimer's Disease Neuroimaging Initiative, 2014. Multi-atlas segmentation of the whole hippocampus and subfields using multiple automatically generated templates. Neuroimage 101, 494–512. <https://doi.org/10.1016/j.neuroimage.2014.04.054>.
- Puonti, O., Iglesias, J.E., Van Leemput, K., 2016. Fast and sequence-adaptive whole-brain segmentation using parametric Bayesian modeling. Neuroimage 143, 235–249. <https://doi.org/10.1016/j.neuroimage.2016.09.011>.
- Ruigrok, A.N.V., Salimi-Khorshidi, G., Lai, M.-C., Baron-Cohen, S., Lombardo, M.V., Tait, R.J., Suckling, J., 2014. A meta-analysis of sex differences in human brain structure. Neurosci. Biobehav. Rev. 39, 34–50. <https://doi.org/10.1016/j.neubiorev.2013.12.004>.
- Russell, M.B., Olesen, J., 1996. A nosographic analysis of the migraine aura in a general population. Brain 119 (Pt 2), 355–361.
- Russo, Antonio, Tessitore, Alessandro, Silvestro, Marcello, Di Nardo, Federica, Trojsi, Francesca, Del Santo, Teresa, De Micco, Rosa, Esposito, Fabrizio, Tedeschi, Gioacchino, 2019. Advanced visual network and cerebellar hyperresponsiveness to trigeminal nociception in migraine with aura. J. Headache Pain 20 (1). <https://doi.org/10.1186/s10194-019-1002-3>.
- Scheltens, P., Barkhof, F., Leys, D., Pruvo, J.P., Nauta, J.J., Vermersch, P., et al., 1993. A semiquantitative rating scale for the assessment of signal hyperintensities on magnetic resonance imaging. J. Neurol. Sci. 114, 7–12.
- Shin, Kyong Jin, Lee, Ho-Joon, Park, Kang Min, 2019. Alterations of individual thalamic nuclei volumes in patients with migraine. J. Headache Pain 20 (1). <https://doi.org/10.1186/s10194-019-1063-3>.
- Skytthe, A., Kyvik, K., Bathum, L., Holm, N., Vaupel, J.W., Christensen, K., 2006. The Danish Twin Registry in the new millennium. Twin. Res. Hum. Genet. 9, 763–771. <https://doi.org/10.1375/183242706779462732>.
- Younis, S., Hougaard, A., Nosedà, R., Ashina, M., 2018. Current understanding of thalamic structure and function in migraine. Cephalalgia 033310241879159. <https://doi.org/10.1016/j.expneurol.2017.03.024>.